

# Flow Dynamics in the Human Carotid Artery: I. Preliminary Observations Using a Transparent Elastic Model

Charles W. Kerber<sup>1</sup> and Carl B. Heilman<sup>2</sup>

**Purpose:** We developed an elastic, transparent, life-size model of the cranial vessels that allowed us to visualize carotid artery flows directly, and wish to report our observations and recorded data. **Materials and Methods:** The brachiocephalic arteries of 12 adult cadavers were cannulated and infused with acrylic. The heads were dissolved in alkali and, using a "lost wax" technique, a silicone model that reflected the shape and size of the original artery was produced. These models were connected to a closed circuit of flowing fluid. The fluid was rendered opaque by injecting isobaric dyes at various points in the streams. **Results:** These dye opacified slipstreams showed a relatively low flow area visible in the posterior and lateral aspect of the carotid bulb that acted as an internal buffer, and directed the more posterior lateral slipstreams anteriorly and at the same time increased their velocity. The cervical internal carotid artery was relatively straight and showed flow patterns that were essentially laminar. In the petrous internal carotid artery, the dye-opacified slipstreams began a helical flow pattern, and areas of flow reversal became apparent along the inner aspect (lesser curvature) of the bend. The central slipstreams tended to flow in a straighter line, passing close to, and sometimes striking the wall of, the outer portion (greater curvature) of the bend. In the cavernous internal carotid artery, helical flow continued. The central slipstreams struck the outer surface (greater curve) of the arterial bend. The point that the central slipstream struck the wall was more distal during systole than during diastole. At the supraclinoid section laminar flow again became established. Certain slipstreams selectively entered individual cranial branches. **Conclusion:** The model we describe should allow more accurate study of complicated flow dynamics in vessels supplying the brain.

**Index terms:** Blood, flow dynamics; Arteries, carotid; Models, anatomic

AJNR 13:173-180, January/February 1992

Since Moniz's (1) classic 1927 monograph describing carotid arteriography, the cerebral angiogram has developed into an accurate and elegant delineator of vascular anatomy. As the technique has evolved, we have unconsciously come to expect it to provide other, more physiologic information. We often attempt to derive flow data: such as when we assign significance to degrees of stenosis caused by carotid atherosclerosis, when we grade the extent of occlusion of arteriovenous malformations after embolic therapy, or

when we assign significance to vasospasm occurring after subarachnoid hemorrhage.

The status of the blood flowing to the brain is of absolute consequence to the organism, as the brain tolerates ischemia poorly. However, it is generally difficult to study flows in the human, particularly in the carotid and vertebral systems. These vessels lie in bone for much of their course and change direction frequently.

We have recently developed an elastic, transparent, life-size model of the cranial vessels (2). Using this model, we have recorded and observed pulsatile and steady flows and wish to communicate our preliminary observations.

## Materials and Methods

Acrylic injections of the brachiocephalic vessels of 12 fresh adult cadavers were made as follows. With the head in a neutral position, the vessels were isolated in the mediastinum, cannulated, and flushed with isotonic saline.

---

Received March 19, 1991; revision requested June 29; revision received August 29; final acceptance September 19.

<sup>1</sup>Department of Radiology and Neurological Surgery, University of California, San Diego Medical Center, H-756, 225 Dickinson Street, San Diego, CA 92103-1990. Address reprint requests to C. W. Kerber.

<sup>2</sup>Department of Neurosurgery, New England Medical Center, 750 Washington Street, Box 267, Boston, MA 02111.

AJNR 13:173-180, Jan/Feb 1992 0195-6108/92/1301-0173

© American Society of Neuroradiology

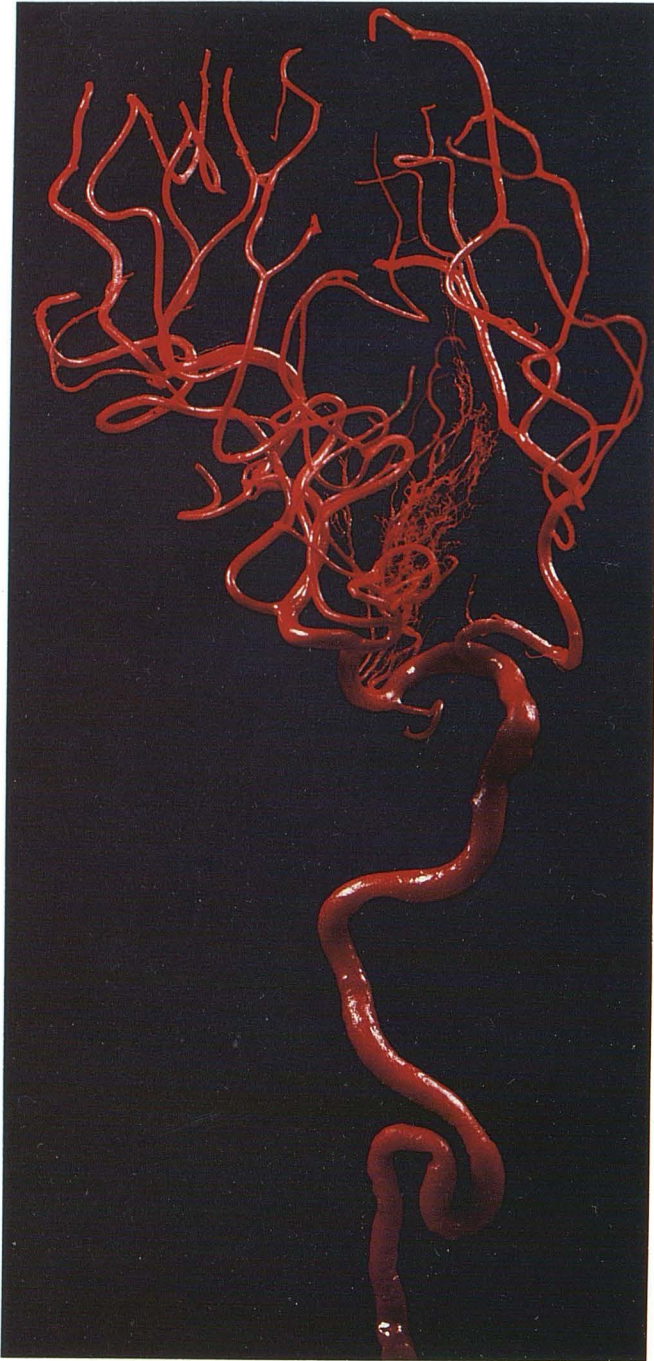


Fig. 1. Frontal view of life-size casting of right internal carotid artery. Note detail obtained; all striate vessels fill. The section of vessel to be studied is generated from a casting like this.

Then, an acrylic casting medium mixed with 100-micron polyvinyl alcohol foam particles was infused. Infusion was stopped when the outer diameter of the common carotid artery reached 9 to 10 mm. When the acrylic polymer had cured, the heads were removed and dissolved in concentrated alkali. What remained were accurate, life-size reproductions of the blood vessels' lumens (Fig. 1). Portions of these lumen castings were then placed into molding ma-

terial. When cured, the molds were opened and the acrylics were discarded. Modeling wax was then infused into the molds and removed when hardened. Those wax impressions reflected to within 1% the original artery's lumen diameter and shape. The wax was covered with an optically clear silicone elastomer, the silicone was cured, and the wax was removed. What remained was a transparent silicone vessel that now was a copy of the original artery. Details of the preparation of the models are reported in another paper (2).

These models were then placed in a circuit of flowing Newtonian fluid. The individual paths or slipstreams of the flowing fluid were made visible by the upstream injection of isobaric food dyes.

Images were recorded on 35-mm film at exposure times between 1/5,000–1/40,000 of a second using an Olympus OM2 camera and 100-mm macro lens, on 16-mm film with a Bolex camera and macro lenses, or with a high-speed, super VHS video camera, 60 frames/sec, with frame exposures between 1/250–1/1,000 of a second. Flow velocities were calculated by measuring the track time of small polyvinyl alcohol particles within the fluid over known distances. Flow volumes were measured instantaneously by a North Carolina Medical Instruments square wave flow meter. The flow meter's accuracy was calibrated by collecting the fluid in a graduated beaker over time.

Both constant and pulsatile flow were studied: constant flow through the circuit was provided by a simple centrifugal pump; pulsatile flow by a modified Harvard apparatus model 1421 heart pump. The Harvard pump allowed control of stroke volume, stroke frequency, and systolic ejection fraction. The flow profile is shown in Figure 2. For these experiments, the fluid used was isotonic saline.

Viscosities were measured on a Brookfield cone/plate viscometer.

Flow was visualized at Reynolds numbers ( $Re$ ) of 100 and 200. In the model, using saline, this corresponded to a flow volume of about 200 mL/min.

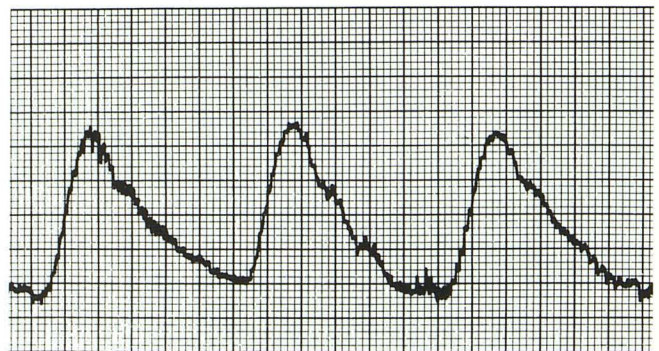


Fig. 2. Flow (not velocity) profile in the pulsatile system. The magnetic sensor is placed just proximal to a 20-cm rigid tube leading into the elastic model. Diastolic flow is about 30% of peak systolic flow.

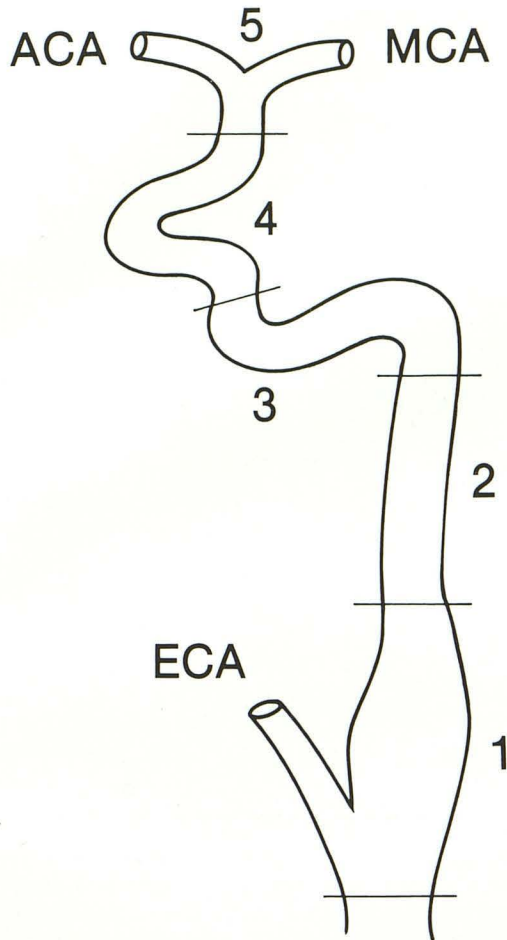


Fig. 3. Line drawing of divisions of the internal carotid artery.

*Segment 1*, the bulb, includes the distal 2–4 cm of the common carotid artery, the bulbous dilatation of the internal carotid artery origin, a 2- to 4-cm segment beyond it or the proximal 2–4 cm of external carotid artery (less the superior thyroid artery). We assumed that 25%–30% of the total flow entered the external carotid artery.

*Segment 2*, the cervical portion. Unlike most other human arteries, this segment typically has neither narrowings nor dilations, almost never branches, and does not taper. It runs cranially (in healthy adults) in a generally straight or slightly serpentine fashion.

*Segment 3*, the petrous portion. The artery makes a right angle bend to pass medially and slightly anteriorly ( $10^{\circ}$ – $20^{\circ}$  to the coronal suture). It then ends in another right-angle bend cranially, and becomes a short straight vessel before merging into the cavernous section.

*Segment 4*, the cavernous internal carotid artery. The vessel begins an anterior  $90^{\circ}$  bend, but immediately curves superiorly and then posteriorly into a C shape. It ends in another  $90^{\circ}$  bend as it turns cranially to enter the subarachnoid space. Its orientation lies in the sagittal plane.

*Segment 5*, the subarachnoid portion. Several small arteries originate as T junctions at nearly right angles to the gently curving artery's tangent. These are the ophthalmic, the posterior cerebral, and anterior choroidal arteries. In most cadavers, the main line continuation of most flow is into the middle cerebral artery, with the anterior cerebral acting almost as a T junction rather than a symmetrical bifurcation.

## Results

We divided the internal carotid artery into five sections having relatively arbitrary boundaries (see Fig. 3).

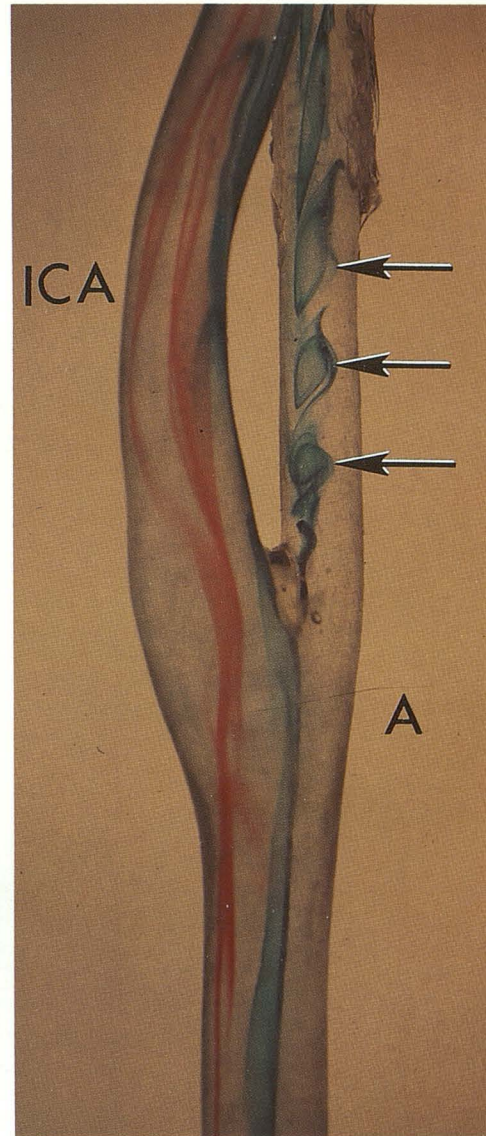


Fig. 4. Lateral view, right carotid bulb; A = anterior. The central (blue) slipstream strikes the carina with a portion passing into the anterior most portion of the internal carotid artery. The remainder enters into the external carotid branch, strikes a small irregularity that causes eddy shedding downstream (arrows). A relatively stagnant lozenge-shaped volume of fluid in the bulbous dilatation acts as an internal buffer, forcing posterolateral (red) slipstreams anteriorly, and increasing their flow velocities. Beyond this relatively stagnant region, the slipstreams pass again toward the posterior wall to reestablish normal laminar flow.

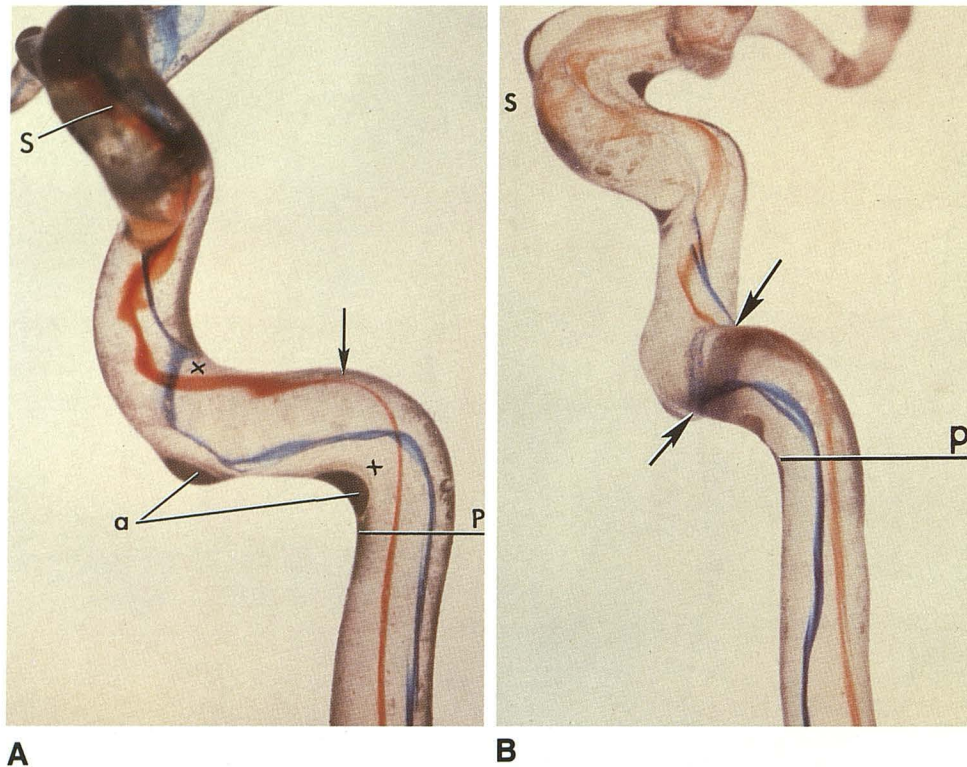


Fig. 5. Left cervical and petrous internal carotid artery.

A, An almost direct anteroposterior view of the cervical and petrous portion. The petrous portion begins at line *P*. Beyond the bulb, laminar flow has become reestablished. Any irregularities caused by bulb abnormalities are quickly dampened in this cervical region. As the artery enters the petrous bone (*P*), it makes slightly greater than a right angle bend and passes medially, horizontally, and anteriorly ( $10^{\circ}$ – $20^{\circ}$  forward of the coronal suture). In this petrous region, a helical flow develops, counterclockwise in this left artery. At the X's, flow reversal is visible during systole. The most central slipstreams strike the distal wall at the point of the *arrowhead*. This point moves slightly, depending upon the phase of the cardiac cycle, with a more distal strike at peak systole. More distally, as the intrapetrous internal carotid artery makes its second right angle bend cranially, the helical flow pattern continues. Central slipstreams again strike the greater convexity, and flow reversal is visible in the concavity. The areas of flow reversal are more prominent with higher velocities. (*S* = Siphon. Artifacts caused by excessive silicone on the outside of the vessel. Though there is optical distortion, the inner lumen of the vessel is unaffected.)

B, Lateral view of same vessel (Siphon, to viewer's left). As different slipstreams are opacified, one appreciates the helical swirling better. Note especially the course of the more anterior (blue) dye path. At lowest arrow it strikes the convexity of the cranial curve, continues to rotate, strikes the posterior wall (*upper arrow*), then continues cranially into the siphon.

### *The Common Carotid Artery Bifurcation*

The most anterior slipstreams passed into the external carotid artery. More central slipstreams consistently struck the carina of the bifurcation and then split, passing into the two branches (Fig. 4). The posterior lateral portion of the bulb contained a relatively stagnant lozenge-shaped area of either slowly flowing fluid or fluid having generally reversed flow. This posterior fluid region acted, at least during systole, as an unwallled internal buffer. When dyes were injected along the posterior aspect of the common carotid artery upstream from the bifurcation, this internal buffer forced most of the slipstream away from the buffer, causing it to pass more anteriorly and increasing its velocity. Some mixing occurred,

and slowly, the fluid in the stagnant area entered the faster slipstreams and was washed away.

The specimen shown in Figure 4 was nearly normal, but did have a slight irregularity at the carina. That minor abnormality created eddy shedding (see Appendix) downstream into the external carotid artery.

### *The Cervical Portion*

In this segment, normal laminar flow established itself quickly after the disturbance seen in the bulb (Figs. 4 and 5). Posterior slipstreams, having been displaced anteriorly in the bulb, returned to a more posterior location, and their velocity decreased.



Fig. 6. Lateral view, left cavernous internal carotid artery. The helical flow becomes even more apparent in this image. Areas of flow reversal are shown by the *arrows*. The central slipstreams strike the convexity of the siphon; the position of the strike changes depending upon the phase of the cycle.

### *The Petrous Portion*

As fluid entered this segment, flow became more complex. The more central slipstreams began to curve anteriorly, but less than that of the model's curve radius, and struck the greater curvature (convexity) of the vessel wall. A helical flow pattern in the slipstreams became apparent. During systole a small area of flow reversal appeared and was located adjacent to the wall about  $\frac{1}{2}$  vessel diameter beyond the lesser curve and was about  $\frac{1}{3}$ – $\frac{1}{2}$  vessel diameter long. In the horizontal section of this artery segment, helical flow continued and persisted as the artery made its second nearly right-angle bend cranially to pass into the entry zone of cavernous carotid artery.

### *The Cavernous Portion*

In this portion, disturbed helical flow continued. The more central slipstreams struck the most anterior portion of the artery (the greater curve wall). During systole, flow reversal was seen in the concavity of the bend (the lesser curve). The area of flow reversal lay about  $\frac{1}{4}$  vessel diameter

downstream from the lesser curve and extended into the central portion of the lumen about  $\frac{1}{4}$  to  $\frac{1}{3}$  the vessel diameter (Fig. 6).

### *The Supraclinoid Portion*

Here, slipstream patterns had an appearance similar to that of the cervical portion and appeared laminar. Flow into the bifurcation was uncomplicated, with the majority of the flow passing into the more directly aligned middle cerebral artery. Some slipstreams, those passing into the anterior cerebral branch, exit at nearly right angles from the main flow. There was almost no flow along the anterior-most aspect of the anterior cerebral artery limb (see Fig. 7). We did not study the effect of other T branches (ie, the ophthalmic, the striates, or the choroidal vessels) in this preliminary report.

### **Discussion**

With the superbly detailed angiograms routinely available today, it is not surprising that we unconsciously attempt to extract physiologic flow data from angiographic images. But the angiogram demonstrates only anatomy. Although that anatomy is important, it is flow that we must understand if we are to analyze the effects of our treatments, recognize the general health of the brain, and discover those patients whose altered flows place them at risk for disease. For example, Stehbens (3), in an excellent and provocative review paper, argues conclusively that aneurysms are not the product of a congenital wall weakness, but rather are degenerative. Certainly, in our observations, the central slipstreams strike the carina of the bifurcations vigorously. As the blood has mass and thus inertia, it is not unreasonable to expect that degeneration would take place at that point.

Studying flow in the carotid arteries has, in the past, been physically difficult. The carotid artery contains an unusually large number of bends, has a focal dilation, changes course repeatedly, and is, for most of its course, not tapered. Vessels elsewhere generally lead directly to their end organ, taper gently, and branch frequently. Further complicating the matter, the basic principles governing flowing fluids are foreign to most clinical physicians. Liepsch has presented clear, concise reviews that will be of practical value for radiologists (4, 5).

The silicone model of the carotid artery does allow an unhurried and safe way to visualize flows

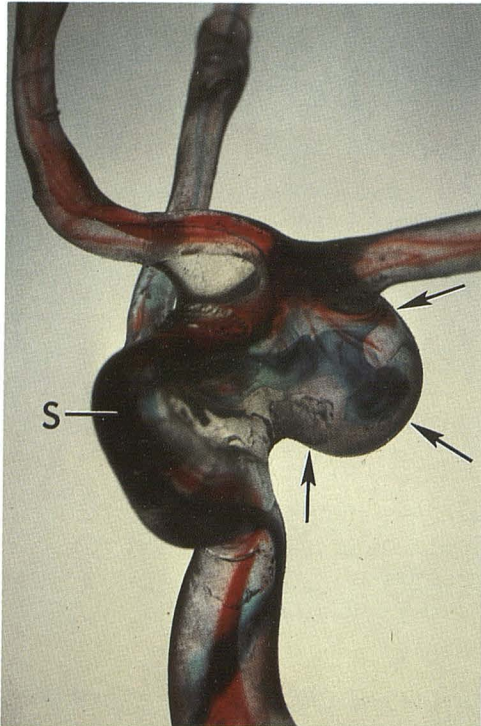


Fig. 7. Frontal view, left internal carotid artery. A large broad necked posterior communicating artery aneurysm is present (arrows). Note the coherence of slipstreams despite the chaotic flow within the aneurysm. The proximally injected red slipstream passes preferentially into anterior and middle cerebral arteries, whereas the blue slipstream, having exited from the aneurysm, passes into the posterior communicating artery. Re about 50; S = siphon.

directly in this complicated vessel. Using appropriate fluids, reasonable physiologic understanding can be achieved. In the model, we used analog methods—global observations—to develop insights and to make basic observations. Watching the flow of the colored dyes gives an almost immediate appreciation of the whole of the fluid dynamics, and replaying the television tape over and over again clarifies areas of doubt.

Dividing the vessel into the arbitrary segments is of value only for descriptive purposes; one can understand the flow only by seeing the whole. The division between cavernous and petrous carotid artery is unimportant from a dynamical flow standpoint, inasmuch as the names are based upon structures that are external to and do not modify the flow.

Although there was eddy shedding visible at our most normal common carotid bifurcation, no real turbulence was evident in any of our models. Flow was consistently channeled away from the posterior dilatation of the bulb. That dilatation held both particles and dyes, sometimes for many seconds, before there was exchange into the

more rapidly flowing medial slip streams. This important area, the primary site of much atherosclerosis, has been elegantly studied by Ku (6), Karino and coworkers (7), and by Motomiya and Karino (8). Perhaps the most physiologically significant finding was that the stagnant or reversed flow area in the posterior bulb acted as an internal dam or buffer, channeling the central and most posterior slipstreams toward the carina, anteriorly. The buffer narrowed the effective channel, and increased the speed of the fluid through this section. This could lead to apparent and factitious narrowing of the channel on magnetic resonance (MR) scans.

Flow in the cervical carotid artery was laminar, not unexpected in light of our use of a Newtonian fluid.

In the petrous portion, flow became complex, but there was no turbulence per se. The flow became helical. This type of flow is difficult to characterize with words, but Liepsch (D. W. Liepsch, personal communication) recommends the descriptive term "highly disturbed" rather than the commonly used word "turbulent." These altered slipstreams retain their character and appearance for many vessel diameters downstream from the bend. The central slipstreams strike the far wall beyond the bend's convex portion (greater curvature). The location of that impact zone varies with the flow velocity, striking more distally with higher velocities (ie, during systole). In the concave (lesser curve) region, we found areas of actual flow reversal. Thus, not only was there a helical flow pattern of the slipstreams along the longitudinal axis of the artery; some of the slipstreams changed course in the most concave portion of the bend, passed proximally for about a  $\frac{1}{3}$  or  $\frac{1}{4}$  vessel diameter, and then curved around again to enter the more rapidly flowing slipstreams. These changes were most evident during the maximum systolic flow.

A similar pattern was visible in the intracavernous segment. The helical flow continued but was dampened somewhat. The slipstreams having the greatest velocity struck the anterior wall of the vessel (the convexity) then continued to swirl into the next bend. Again, along the lesser curve wall, some flow reversal was evident at higher velocities. As the flow passed into the supraclinoid internal carotid artery, disturbances became dampened resulting in more laminar flow with the majority of the flow continuing into the middle cerebral artery branch. The anterior cerebral artery received approximately 20% of the

flow in most models. The central slipstreams struck the carina with some vigor.

Aside from our need to see and describe the basic physiology and pathology of flow in this important vessel, there are two practical considerations that might be addressed with these models. The first of these is the importance of slipstream rheology during the angiographic delivery of a chemotherapeutic agent. Figure 7 shows that, although the isobaric fluid has been injected some 30 or 40 vessel diameters proximally, the coherence of the slipstreams has caused the blue dye to enter the posterior communicating artery selectively. Unless the angiographer proves that mixing is occurring with a given infusion rate, one should assume it is not, and that streaming is carrying the agent to vessels determined by the system's innate rheologic property. The good mixing of contrast agent with blood during the diagnostic angiogram may not reflect the rheologic character of a slower flow injection.

The second consideration is in the important and rapidly expanding field of MR angiography. MR imaging unfortunately is associated with a myriad of artifacts, and flowing fluids are particularly troublesome. Even now, in gradient recalled images, one can see evidence of these flowing slipstreams and see their effect in the images. Unless the slipstreams are well understood, MR angiography may be so fraught with artifacts that our clinical colleagues may not appreciate its potential. Fortunately, these models are MR compatible.

In summary, the model has proven itself to be an efficacious way to visualize flow in the human internal carotid artery. Though those flows are complex, there is order in the apparent chaos. We found no true turbulence in our nearly healthy specimens. We believe the model will allow a more accurate study of the complicated flow dynamics of the vessels supplying the brain. It is now being used to correlate the many changes seen on current MR studies with normal and pathologic states.

Unfortunately, the static images shown here cannot convey the elegance, the beauty, and the complexity of the dynamic flows one sees on motion recordings.

## Acknowledgments

The authors wish to thank Kim Lee for preparation of the molds, and Ramona Garcia and Esther Avery for the manuscript preparation.

## Appendix

### *Bifurcations*

Vessel branch points. Branches, or daughter limbs may exit from the parent symmetrically, such as we see in the distal aorta, or they may exit at varying angles from the main vessel, such as the ophthalmic artery and the superior thyroid artery. If they exit at approximately right angles, they are often referred to as T junctions.

### *Biorheology*

The study of flowing fluids in living organisms.

### *Eddy shedding*

The production of swirls by an eccentric projection into the stream. The eddies (swirls) gradually become dampened out as they pass downstream. They are usually associated with bruits.

### *Flow, laminar*

The efficient passage of fluid through a pipe. This passage is best thought of as concentric sleeves of fluid which flow faster and faster the closer they are to the center of the tube. Adjacent to the wall there is, for all practical purposes, no flow (the no-slip area). As one moves toward the center of the lumen, away from the wall, the velocity of the flowing sleeves increases rapidly. (The thin outer area is called the boundary layer). If one plots the velocity vectors of the flowing fluid, they form a parabola. The human common carotid artery, at least on ultrasound exam, does not show laminar flow.

### *Flow, turbulent*

Inefficient fluid passage through a tube caused by breakup of the smooth flowing slipstreams. Remarkable energy losses occur when turbulence begins. Flow into the base pool of a waterfall is a good example.

### *Flow, disturbed*

These are poorly described flows that occur at the junction point between laminar and turbulent flow. These conditions are often found in the human body. Two different types may be described:

- a. *Periodic disturbed flow* is seen when a partial obstruction is placed into a slipstream such as an eccentric atherosclerotic plaque (see Fig. 4). Eddies form downstream from the plaque. These eddies become dampened out as they pass further and further away from the point of obstruction. See *eddy shedding*.
- b. *Disturbed chaotic flow*. Chaotic appearing flow, as in an aneurysm, but with an order to the chaos. Slipstreams are disordered, swirl, and there may be areas of flow reversal along portions of the tube.

### Flow profile

A pictorial representation of the velocity vectors of flowing fluid. One can obtain these in live humans with doppler ultrasound. In Newtonian fluids a line drawn along the leading edge of the velocity vectors forms a parabola. In the normal human common carotid artery, however, within a millimeter of the artery's wall, the velocity vectors become relatively constant, and the profile goes from nearly zero to essentially terminal velocity (about 60 to 80 cm/sec at peak systole).

### Reynolds number

Abbreviated Re, the Reynolds number is a dimensionless comparison of viscous to inertial forces in a specific fluid system. Actual calculation of the number depends upon the viscosity of the fluid, the diameter of the tube, and the velocity of the fluid flow. A swimming whale for example, has a Reynolds number of about 300 million. Blood at peak flow in the carotid artery has an Re of about 200, while a capillary's Re is about 1. A motile sperm has an Re of about 0.01. At lower numbers, as in capillaries, viscous forces are prominent. In the carotid artery, inertial forces are more prominent.

### Newtonian fluid

A liquid such as water or isotonic saline, or a gas, such as air, that has no memory for prior events. The viscosity

of a Newtonian fluid remains constant even if it changes velocity, ie, has a varying shear force placed upon it. Blood is not Newtonian. When sheared (as when it passes a partial obstruction or turns a bend) its viscosity decreases because the rouleaux break up. Smaller blood aggregates have less viscosity. The most common example of a non-Newtonian fluid (other than blood) would be slime or ketchup. Both change viscosity when they begin to flow.

### References

1. Moniz, E. L'Encephalographie arterielle, son importance dans localisation des tumeurs cerebrales. *Rev Neurol* 1927;3:72-90
2. Kerber CW, Heilman CD, Zanetti PH. Transparent elastic arterial models. I. A brief technical note. *Biorheology* 1989;26:1041-1049
3. Stehbens WE. The etiology of intracranial berry aneurysm. *J Neurosurg* 1989;70:823-831
4. Liepsch DW. Flow in tubes and arteries: a comparison. *Biorheology* 1986;23:395-433
5. Liepsch DW, Morabec ST. Pulsatile flow of non-Newtonian fluid in distensible models of human arteries. *Biorheology* 1984;21:571-586
6. Ku DN, Giddens DP. Pulsatile flow in a model carotid bifurcation. *Atherosclerosis* 1983;3:31-39
7. Karino T, Motomiya M. Flow visualization in isolated transparent natural blood vessels. *Biorheology* 1983;20:119-127
8. Motomiya M. and Karino T. Flow patterns in the human carotid artery bifurcation. *Stroke* 1984;15(1):50-56